Influence of Pole-pair Combinations on the Characteristics of the Brushless Doubly Fed Induction Generator

Ashnaz Oraee, *Member, IEEE,* Richard McMahon, Ehsan Abdi, *Senior Member, IEEE*, Salman Abdi, *Member, IEEE,* and Sul Ademi, *Member, IEEE,*

***Abstract*—The brushless doubly fed induction generator (BDFIG) is an alternative to the doubly fed induction generator (DFIG), widely used in wind turbines which avoids the need for brush gear and slip rings. The choice of pole numbers for the two stator windings present in the BDFIG sets the operating speed desired to be in the medium speed range to eliminate a gearbox stage. However, the choice of pole number also affects the torque capability, magnetizing currents and back iron depth. In addition, some pole pair combinations may introduce undesired direct coupling between the two stator windings and unbalanced magnetic pull and vibration. Analytical expressions are developed for these effects and a comparison is made between the BDFIG and the conventional DFIG. The torque capabilities and magnetizing currents are not strongly dependent on the choice of pole numbers but the back iron depth is significantly affected. The torque density of the BDFIG is somewhat reduced compared to a similarly sized DFIG but magnetizing currents per unit torque are the same. However, the required back iron depths are greater. The work also shows that multi-megawatt machines are expected to work within the desired range of power factors at acceptable efficiencies.**

***Index Terms*—Brushless doubly-fed generator (BDFG), electrical machine design, induction generator, power factor, pole-pair.**

List of Symbols

p_1, p_2	stator winding pole pairs (principal fields)
g	airgap length
$n_r, n_{r_{opt}}$	rotor turns ratio general and optimal
f, f_1, f_2	frequency stator windings 1,2
l, d	stack length, air gap diameter
ω_r	rotor angular velocity
B_1, B_2	RMS value of flux density stator windings 1,2
N_1, N_2	number of turns stator windings 1,2
B_c	peak flux density in core
y_c	back iron depth
ω_r	rotor angular velocity
B_{sum}, B_{quad}	sum and quadrature sum of flux density stator windings 1,2
$\bar{B}$	magnetic loading
$\bar{J}$	electric loading

I. Introduction

THE brushless DFIG is an alternative to the well-established Doubly Fed Induction Generator (DFIG) for use in wind turbines since it offers improved reliability and reduced capital and maintenance costs [1]. It retains the low-cost advantage of the DFIG system as it only requires a fractionally rated converter and does not use permanent magnet materials. The machine has no brushed contact to the rotor, eliminating a common source of failures, making it a particularly attractive machine for offshore wind turbines. In addition, the brushless DFIG is intrinsically a medium-speed machine, enabling the use of a simplified one or two stage gearbox. A schematic of the brushless DFIG drivetrain is shown in Fig. 1. The brushless DFIG has its origins in the self-cascaded machine and has two non-coupling stator windings, referred to as the power winding (PW) and the control winding (CW) with different pole numbers, p_1 and p_2. creating two stator fields in the machine's magnetic circuit with different frequencies and pole numbers [2]. A specially designed rotor couples to both stator windings.

Other applications than wind power have also been considered for the brushless DFIG, for instance, a stand-alone generator for off-grid applications [3], a drive in pump applications [4], [5], a synchronous compensator and a ship drive [6]. In addition, the brushless doubly fed reluctance machine (BDFRM) has been widely taken into consideration and several design modifications and control optimisations have been proposed for example in [7], [8].

The design of the brushless DFIG is not straightforward since there are more variables to consider than in conventional induction machine designs [9]. Attention has been given to some aspects of design for wind power applications as reported in [10]–[13] and several large machines reported. These include the 75 kW machine [12], the 200 kW machine [14] and the 250 kW machine built and tested by the authors of [15]. This latter, believed to be the largest to date, was conceived as a stepping-stone towards commercial MW scale brushless DFIGs.

In a wind turbine application, the machine will be matched to the rest of the drive train so the natural speed, dependent on the sum of the pole-pairs, and the speed range around natural speed, typically $\pm 30\%$, are of interest. This paper looks at how the design and performance of the machine is affected by the choice of pole-pairs, and the allocation of these to the two windings. Machine characteristics examined include pull-out torque, back iron depth and magnetizing current.

It was shown in [17] that to achieve the required performance for wind turbine service, namely a power factor in the range of 0.95 lag to 0.95 lead, the CW of the brushless DFIG considered needed to be significantly over-

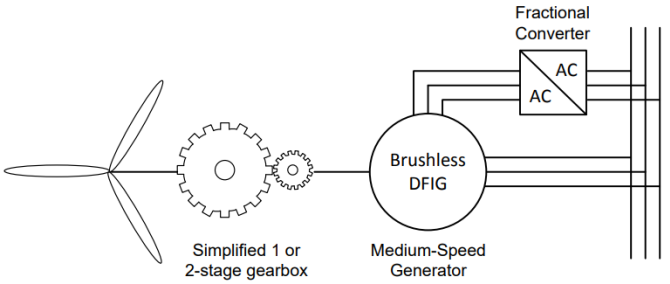

Fig. 1: Brushless DFIG drivetrain set-up for wind power applications.

excited, compromising machine output. The rotor leakage inductance is particularly significant in setting the degree of over-excitation needed. The final section of this paper looks at the performance trends of future medium-speed MW scale brushless DFIGs.

To control and ensure stability of the brushless DFIG, the presence of two stator windings means that there are more variables to consider than in a single winding machine. Performance of the system dynamics, control and stability and Low Voltage Ride Through (LVRT), has been greatly investigated in [15] and [Reference P.Roberts Paper Dynamic modelling of the brushless doubly fed machine].

This paper is organized as follows. Section II describes the brushless DFIG operation and the per-phase equivalent circuit. The pole-number choice and effect on machine rating are presented in section III. The effect of pole-pair split on machine fields and back-iron considerations are reported in section IV. Section V details the amp-turns ratios for common (p_1/p_2) pole-pair. Performance analysis of the 4/8 frame size of the D400 prototype, the pull-out torque, power factor and efficiency are detailed in section VI. Optimization design for the megawatt (MW) brushless DFIGs are explored and brought into focus in Section VII. Finally, Section VIII draws vital conclusions of this paper.

II. Brushless DFIG Operation

The BDFIG normally operates in the synchronous mode in which the shaft speed is independent of the torque exerted on the machine, as long as it is smaller than the pull-out torque. The speed is determined by the frequency and pole-pair numbers of the stator windings and is given by:

$$N_r = \frac{60(f_1 + f_2)}{p_1 \pm p_2} \tag{1}$$

where f_1 and f_2 are the frequencies of the supplies to the stator windings, p_1 and p_2 are the pole-pair numbers of the windings.

A. Brushless DFIG equivalent circuit

The operation of the BDFG can be described by a per-phase equivalent circuit [17] similar to the equivalent circuits of two induction machines with interconnected rotors, as shown in Fig. 2. In the figure R_1 and R_2 are the stator resistances, L_{m1} and L_{m2} are the stator magnetizing inductances and L_1 and L_2 are the stator leakage inductances. Parameters are referred to the PW using the modifier '′'. Furthermore, the rotor can be characterized by the rotor turns ratio n_r, resistance R_r and leakage inductance L_r, the two latter parameters are also shown in the referred per-phase equivalent circuit of Fig. 2.

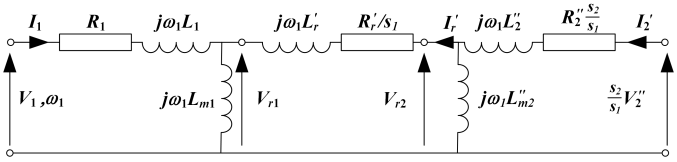

Fig. 2: Referred per-phase equivalent circuit of the brushless DFIG.

The rotor leakage inductance includes conventional leakage elements but the space harmonics associated with common designs of brushless DFIG rotors lead to a higher differential leakage component compared to conventional induction machine rotors. The slips s_1 and s_2 are defined as in [1].

III. Pole-Number Choice

A. Choice of pole numbers

For $(p_1 + p_2)$ type brushless DFIGs, the choice of stator winding pole-pair numbers to give a desired natural speed, hence operating speed range, is the first step in the design process. The sum of the pole-pair combination, rounded to the nearest integer, is given by:

$$p_1 + p_2 = \frac{60 f_1}{N_r} \tag{2}$$

Both the total pole-pair count and the split between the windings affect machine performance. Direct coupling between the two stator windings must be avoided and this can be achieved by applying the rules given in [18]. In some cases, several pole number combinations are possible and there is the choice of giving the higher or lower pole number to the PW. The torque capability of a brushless DFIG collapses as the speed of the machine approaches the synchronous speed of the PW. Thus, for the widest speed range, the lower pole number should be assigned to the PW. However, if the operating speed range is limited to $\pm 30\%$ around natural speed, as in wind power applications, this constraint does not apply and the frequency of the rotor currents is reduced in this connection. Furthermore, some pole pair combinations may lead to unwanted unbalanced magnet pull and vibration effects. When there is more than one permissible combination of pole pair numbers, machine design can be modified to give optimal performance which is a trade off between output torque, speed, and magnetization considerations to determine the most appropriate combination.

B. Effect on machine rating

An expression for the power rating of the brushless DFIG, calculated from the equivalent circuit model, was derived in [1]. This expression was based on the quadrature sum (B_{quad})

of the two fields in the machine but an alternative approach taking a more conservative view of the maximum allowable fields was developed in [18] based on the simple sum of the fields. Both relationships are given in A. Unfortunately, there is at present no easy way of determining the maximum tolerable fields in the machine but experience suggests that B_{sum} is too conservative [19]. The two assumptions do, however, appear in practice to bracket the range of allowable flux densities so both are considered. Certain other assumptions are used in the expressions for power rating, the most relevant here is that are that only synchronous torques are produced and that the voltage drop across the rotor is not significant.

As the output power is proportional to speed it is instructive to normalize the output of the brushless DFIG to that of a DFIG with a synchronous speed equal to the natural speed of the brushless DFIG, both machines having the same rotor dimensions. The induction machine therefore has (p_1+p_2) poles [20]. This leads to expressions for the output factor, in effect the ratio of available torque to that of the equivalent DFIG, again as derived in Appendix A. The expression depends on the rotor turns ratio n_r but can be evaluated using a value equal to the optimum value as given in Appendix A, in the case of the simple sum basis it reduces to:

$$Output factor = \frac{T_{BDFM}}{T_{IM}} = \frac{1+\frac{p_2}{p_1}}{(1+(\frac{p_2}{p_1})^{\frac{1}{2}})^2} \tag{3}$$

The corresponding expression based on the quadrature sum method is:

$$Output factor = \frac{T_{BDFM}}{T_{IM}} = \frac{1+\frac{p_2}{p_1}}{(1+(\frac{p_2}{p_1})^{\frac{2}{3}})^{\frac{3}{2}}} \tag{4}$$

The output factors for common (p_1/p_2) brushless DFIGs are given in Tab. I, showing that the higher the ratio of pole numbers the greater the output factors can be obtained. This implies that the relative output is a minimum when $p_1 = p_2$, recognizing that such a machine is impractical, as noted in [21]. Using the sum of fields assumption, the minimum output torque is 50% of that of a $(p_1 + p_2)$ induction machine but this rises to nearly 54% for the 2/6 pole configuration. For comparison, the quadrature sum method gives substantially higher output factors, as shown in Tab. I.

TABLE I: Output Factor for Various Pole Number for Brushless DFIG

(p_1/p_2)	$n_{r_{opt}}$ (sum)	$n_{r_{opt}}$ $(quad)$	Outpur factor (sum)	Output factor $(quad)$
2/6	0.577	0.48	0.536	0.74
8/12	0.816	0.76	0.505	0.71
4/8	0.707	0.53	0.515	0.72
2/8	0.5	0.40	0.556	0.76
2/10	0.45	0.34	0.573	0.77

IV. Magnetic Circuit Considerations

A. Effect of pole-pair split on machine fields

It was shown in [1] that the two fields in a brushless DFIG mode are related by the rotor turns ratio, pole numbers and voltage drop across the rotor leakage inductance. If it is assumed that this drop is small, then the ratio of the two fields is given by:

$$\frac{B_2}{B_1} = n_r \frac{p_2}{p_1} \tag{5}$$

where B_1 and B_2 are the rms values of the fundamental p_1 and p_2 pole-pair air gap flux densities. However, in reality there can be a significant voltage across the rotor impedance, especially when the machine is over-excited so (5) is no longer valid. Over-excitation is particularly likely in smaller machines to achieve an acceptable grid-side power factor [17].

B. Back iron considerations

The back iron flux in conventional induction machines is defined as half of the total flux over one pole pitch. The peak flux density in stator or rotor core is then related to the magnetic loading by conservation of flux and for the brushless DFIG it can be calculated from:

$$\hat{B}_c = \frac{\sqrt{2}}{2}\frac{d}{py_c}B_{sum} \tag{6}$$

where y_c is the back iron depth. The back iron flux density in the brushless DFIG varies with time and position but a value for the peak can be found using B_{sum} which is divided into B_1 and B_2 for p_1 and p_2 fields, respectively, using equation (5). The back iron depth for the brushless DFIG is then given by [10]:

$$y_c = \frac{\sqrt{2}}{2}\frac{d}{\hat{B}_c}\left[\frac{B_1}{p_1} + \frac{B_2}{p_2}\right] \tag{7}$$

For the brushless DFIG the back-iron depth in terms of the total air gap flux density, B_{sum}, can be found by rearranging and substituting equations (5) and (6) in (7):

$$y_c = \frac{\sqrt{2}}{2}d\frac{B_{sum}}{\hat{B}_c}\left[\frac{p_1(1+\frac{1}{n_r}) + p_2(1+n_r)}{2p_1p_2 + p_2^2n_r + p_1^2\frac{1}{n_r}}\right] \tag{8}$$

Substituting $n_{r_{opt}}$ from equation (23) then gives:

$$y_c = \frac{\sqrt{2}}{2}d\frac{B_{sum}}{\hat{B}_c}\left[\frac{(1+\frac{p_2}{p_1})(1+2(\frac{p_2}{p_1})^{\frac{1}{2}}+\frac{p_2}{p_1})}{2(\frac{p_2}{p_1}) + (\frac{p_2}{p_1})^{\frac{1}{2}} + (\frac{p_2}{p_1})^{\frac{3}{2}}}\right] \tag{9}$$

The back-iron depth ratio of the (p_1/p_2) brushless DFIG to a conventional induction machine of $(p_1 + p_2)$ poles is given by:

$$\frac{y_{c_{BDFM}}}{y_{c_{IM}}} = (p_1) + (p_2)\left[\frac{p_1(1+\frac{1}{n_r}) + p_2(1+n_r)}{2p_1p_2 + p_2^2n_r + p_1^2(\frac{1}{n_r})}\right] \tag{10}$$

A similar approach gives the ratio of back iron depths on the basis of the quadrature sum method, given by:

$$\frac{y_{c_{BDFM}}}{y_{c_{IM}}} = (p_1 + p_2)\left[\frac{p_1(1+\frac{1}{n_r}) + p_2(1+n_r)}{2p_1p_2 + p_2^2 n_r + p_1^2(\frac{1}{n_r})}\right] \quad (11)$$

The back-iron depth ratios for common (p_1/p_2) pole-pair brushless DFIGs have been calculated and are given in Tab. II for both the simple and quadrature sum methods. The peak flux density in the back-iron is limited to 1.8 T. The back-iron ratio is a minimum at $p_1 = p_2$ which is unfeasible, as noted earlier. The minimum depth is twice of that of a $(p_1 + p_2)$ induction machine on the simple sum basis, and $2\sqrt{2}$ times on the quadrature sum basis which, however, gives a higher machine output. As the ratio of pole-pair numbers increases, there is a slight rise in the depth of back iron required.

TABLE II: Back-Iron Ratio for Various Pole Numbers of Brushless DFIG

Brushless DFIG (p_1/p_2)	$n_{r_{opt}}$ (sum)	$n_{r_{opt}}$ $(quad)$	Output factor (sum)	Output factor $(quad)$
2/6	0.577	0.48	2.31	3.37
8/12	0.816	0.76	2.04	3.00
4/8	0.707	0.53	2.12	2.95
2/8	0.5	0.40	2.50	2.69
2/10	0.45	0.34	2.68	2.98

The results for a wide range of pole number combinations on the basis of optimum turns ratio calculation for the sum and quadrature sum method are shown in Fig. 3. The BDFG needs more back iron than a corresponding DFIG as the two machine fields have lower pole numbers but in any case a certain minimum back iron depth may be mandated by structural considerations. To determine an accurate depth requires finite element analysis to take saturation into account [19].

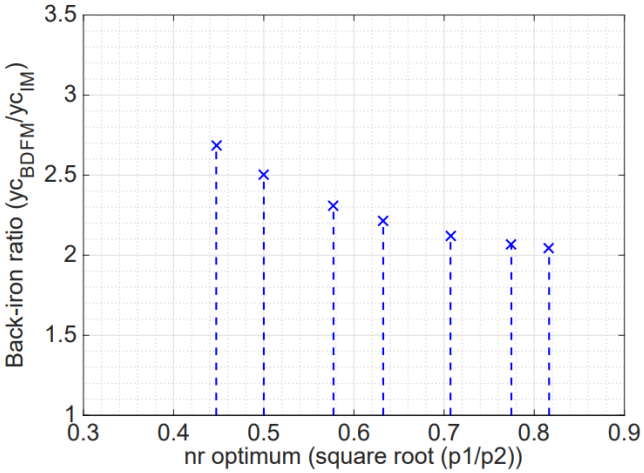

Fig. 3: Back-iron ratio variation with optimum turns ratio.

V. Magnetization

A. Magnetizing amp-turns

For the brushless DFIG the total magnetizing amp-turns (AT_{tot}) for the p_1 and p_2 pole-pair fields, assuming that they are in ratio given by equation (5), are given by:

$$AT_{tot} = \frac{2g}{\mu_o}\frac{\pi}{6}p_1\left[\frac{1+(\frac{p_2}{p_1})^2 n_r}{1+(\frac{p_2}{p_1})n_r}\right] \quad (12)$$

where AT_{tot} is the product of $I_{mag}N_{eff}$, g is the air gap length and μ_o is the permeability of air. The amp-turns ratio of the (p_1/p_2) brushless DFIG to a conventional induction machine of $p_1 + p_2$ pole-pairs is then:

$$\frac{AT_{BDFIG}}{AT_{DFIG}} = \left(\frac{p_1}{p_1+p_2}\right)\left[\frac{1+(\frac{p_2}{p_1})^2 n_r}{1+(\frac{p_2}{p_1})n_r}\right] \quad (13)$$

Substituting $n_{r_{opt}}$ from equation (23) for the B_{sum} formulation gives:

$$\frac{AT_{BDFIG}}{AT_{DFIG}} = \left(\frac{p_1}{p_1+p_2}\right)\left[\frac{1+(\frac{p_2}{p_1})^{\frac{3}{2}}}{1+(\frac{p_2}{p_1})^{\frac{1}{2}}}\right] \quad (14)$$

The corresponding expression for the quadrature sum approach and substituting $n_{r_{opt}}$ from equation (24) is given by:

$$\frac{AT_{BDFIG}}{AT_{DFIG}} = \left(\frac{p_1}{p_1+p_2}\right)\left[\frac{1+(\frac{p_2}{p_1})^{\frac{4}{3}}}{1+(\frac{p_2}{p_1})^{\frac{2}{3}}}\right] \quad (15)$$

The amp-turns ratios for common (p_1/p_2) pole-pair brushless DFIGs are calculated and given in Tab. III. From a magnetizing current point of view, this ratio is a minimum at $p_1 = p_2$ but this is impractical. On the simple sum basis the magnetizing amp-turns are 50% of that of a $(p_1 + p_2)$ induction machine, but the brushless DFIG's torque, according to (18) is only half that of the induction machine, showing that the brushless DFIG requires the same magnetizing AT per unit torque. Similarly, on a quadrature sum basis, the magnetizing AT are 70.7% of those of a DFIG, but again the output torque is only 70.7%. Whilst there is an increase in the magnetizing AT with a greater ratio of pole numbers, there is a corresponding rise in output factor so a (p_1/p_2) BDFG requires essentially the same magnetizing AT as a $(p_1 + p_2)$ DFIG.

TABLE III: Amp-Turns Ratio for Various Pole-Pair Brushless DFIG

Brushless DFIG pole ratio	$n_{r_{opt}}$	Amp-turn ratio (sum)	AT ratio $(quad)$
1/3	0.577	0.567	0.76
2/3	0.816	0.510	0.72
1/2	0.707	0.528	0.73

The amp-turns ratio of the brushless DFIG to the conventional induction machine for various pole-pair ratios using the simple sum method is presented in Fig. 4.

VI. Performance Analysis and Results

The foregoing points are examined in the context of an existing frame size D400, 250 kW brushless DFIG [15] by considering designs for different speed options i.e. pole number combinations. The equivalent circuit model is used to

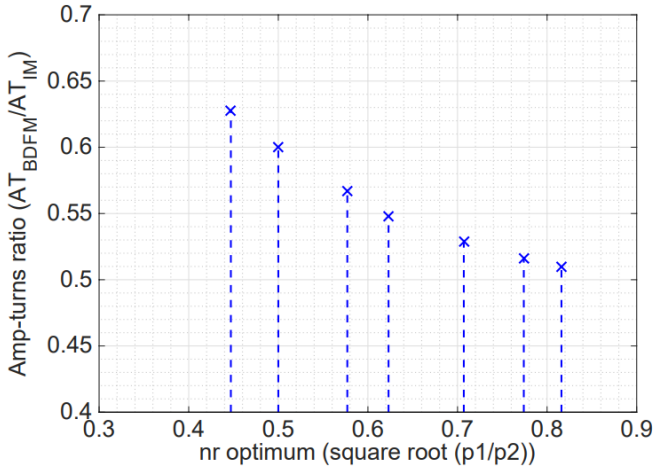

Fig. 4: Amp-turns ratio variation with optimum turns ratio.

represent the steady-state performance of the machine offering a straightforward way of calculating the efficiency and power factor to a practical accuracy. The physical dimensions and specifications of the D400 machine together with stator and rotor winding details are given in Tab. IV.

TABLE IV: Specifications of the 4/8 Frame Size D400 Brushless DFIG

Physical dimentions			
Stack length, mm	820	Rated power, kW	250
Stator diameter, mm	440	Rated torque, Nm	3670
Stator slots	72	Speed range, rpm	500 $\pm$ 36%
Rotor slots	60	Efficiency	93%
Winding details			
PW poles	4	PW rated voltage	690 (50 Hz)
PW turns	48	PW rated current	94 A
CW poles	8	CW rated voltage	620 (18 Hz)
CW turns	168	CW rated current	40 A

The nested-loop rotor of this machine comprises $(p_1+p_2)/2$ sets of nests each with five loops, the conductors being solid bars with one common end ring. The number of rotor slots, and hence the number of loops, will therefore depend on the pole number count and so the machine will not necessarily be suited for actual manufacture.

A. D400 machines

Designs for common brushless DFIG pole-pair combinations using the same dimensions of the existing D400 prototype machine have been investigated. Tab. V provides details of the designs with constant rated torque but different speeds and hence powers. The PW power factor is set to 0.95 lagging, determining the CW voltage and the balance between B_1 and B_2 is changed by varying number of turns. The total flux density, B_{sum}, is 0.7 T and peak flux densities in the rotor tooth and back-iron is limited to 1.5 T. All equivalent circuit parameters, including leakage inductances, are recalculated for each new design using the software described in [18]. The total stator electric loading is kept at 5.7 A/mm. Furthermore, the number and diameter of the stator conductors and cross-section of the rotor bars are modified such that the total conductor cross-sectional areas are identical to those of the D400 machine. The stator current density is 3.5 A/mm^2 and the rotor current density is 5 A/mm^2. The air gap diameter and stack length has been kept constant for all pole number designs.

TABLE V: Design of Various Pole Number Brushless DFIGs for Fixed PW Power Factor of 0.95 Lagging

Brushless DFIG design parameters				
Pole (p_1/p_2)	8/12	4/12	4/8	2/6
ω_n (rpm)	300	375	500	750
Rated power (kW)	150	187	250	375
Rotor slots	100	80	60	56
Stator slots	72	72	72	72
N_1	120	76	66	40
N_2	220	210	146	100
B_1 (T)	0.230	0.271	0.219	0.218
B_2 (T)	0.470	0.429	0.481	0.482
Efficiency	82%	84%	88%	95%
Torque (kNm)	3.7	3.7	3.7	3.7
PW power factor	0.95 lag	0.95 lag	0.95 lag	0.95 lag
Total amp turns	5313	4954	3261	2300

It can be seen that the 2/6 pole brushless DFIG has both the highest natural speed, power and efficiency, whilst producing the same torque as the original 4/8 machine. Furthermore, this pole-pair configuration requires the lowest total amp-turns for magnetization but needs the highest back iron depth shown in Tab. VI.

TABLE VI: Back Iron Design of Various Pole Number Brushless DFIGs

Brushless DFIG pole (p_1/p_2)	n_r	B_1 (T)	B_1 (T)	y_c (mm)
2/6	0.53	0.27	0.43	71
4/8	0.68	0.29	0.41	43
4/12	0.53	0.27	0.43	36
8/12	0.80	0.32	0.38	25

To reduce the depth of back iron, the B_{sum} limit can be increased from 0.7 to 0.8 T while still avoiding saturation effects. Tab. VII shows modifications to the design of the D400 BDFIG for higher B_{sum} for a constant torque of 3670 Nm. The distribution of B_1 and B_2 is calculated using the same method as described earlier in section IV. Due to the change in the number of PW and CW turns the total amp-turns is also changed. In the redesigns, conductor current densities, slot dimensions and slot fill are kept constant. The peak flux densities in the rotor tooth and back-iron are limited to 1.6 and 1.7 T, respectively.

As evident from Tab. VII, unity PW power factor can be achieved at rated design CW voltage of 620 V for the 250 kW brushless DFIG by increasing the total flux density in the air gap. To obtain unity PW power factor for a B_{sum} of 0.75 T and 0.8 T, B_1 is increased by 20% and 14%, respectively.

TABLE VII: Design Optimization of the 4/8 D400 BDFIG for Increased B_{sum}

4/8 D400 BDFIG	B_{sum} = 0.7 T	B_{sum} = 0.75 T	B_{sum} = 0.8 T
B_1 (T)	0.219	0.230	0.250
B_2 (T)	0.481	0.520	0.550
N_1	66	62	57
N_2	146	134	127
Efficiency	88%	89%	90%
PW power factor	0.95 lag	1	1
Total amp turns	3261	3517	3704

B. Pull-out torque of D400 machines

From the previous section, the theoretically available maximum running torque depends to a degree on total pole count and on the split of pole numbers. However, a further consideration is the load angle at which the machine operates, related in turn to the pull-out torque. For well-known reasons, operation away from pull-out is desirable. In the BDFIG the pull-out torque is primarily determined by the rotor inductance and this was believed to increase with pole count [10].

To investigate the effect, brushless DFIGs were designed with the same overall rotor dimensions, starting from the well-characterized 250 kW D400 frame size machine [15], for different pole numbers using the design methodology reported in [18]. The stator windings were configured to use the same number of stator slots and the rotor slots are chosen to give enough conductor area for the stator electrical loading to be balanced, with the same current density in the rotor conductors as the previous section. The design program calculates machine parameters, notably the rotor leakage inductance taking into account space harmonic effects and the couplings between the rotor loops using simple sum analysis method.

Figure. 5, shows the variation of pull-out torque for BDFIGs with different natural speeds in ascending order correspond to 8/12, 4/12, 4/8 and 2/6 pole machines. It can be seen that the 4/8 and 2/6 pole machines with natural speeds of 500 and 750 rpm, respectively, offer somewhat higher pull-out torques allowing easier control and improved stability due to lower rotor leakage inductance, L_r. When designing high pole count machines, there is a need to pay careful attention to keeping the rotor inductance down to an acceptable level to retain a good margin of pull-out torque relative to normal running torque but this is seen to be achievable at least to a total pole count of twenty. The normal running full load torque for designs with natural speeds of 300, 375, 500 and 750 rpm is 3.7 kNm.

C. Power factor

Achieving a good power factor is important and increasingly wind turbines are expected to contribute VArs. The selection of machine speed, and hence pole-pair count has a significant effect on machine operating conditions. Fig. 6 shows variation of the PW power factor for sums of p_1 and p_2 pole-pairs at balanced excitation (minimum rotor currents), preferred for low losses. It can be seen that for brushless DFIGs with a lower sum pole-pairs, higher PW power factors can be achieved. The designs used in Fig. 6 are those in Tab. V, which were designed to be capable of operating at a fixed power factor of 0.95 lagging; parameters are given in Appendix A.

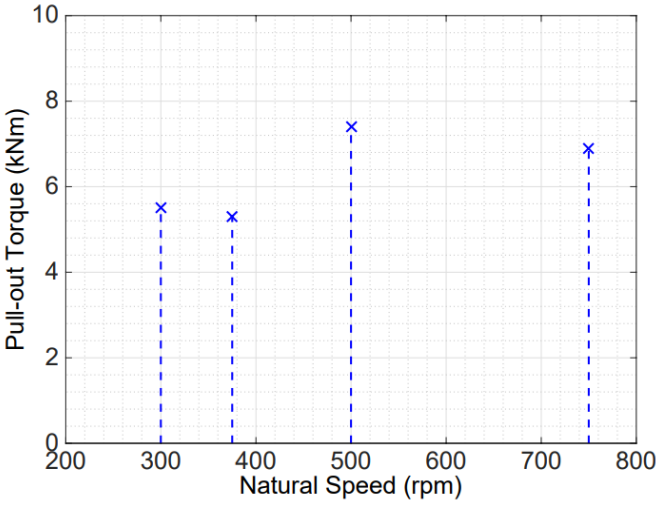

Fig. 5: Pull-out torque variation with natural speed and normal running torque of 3.7 kNm.

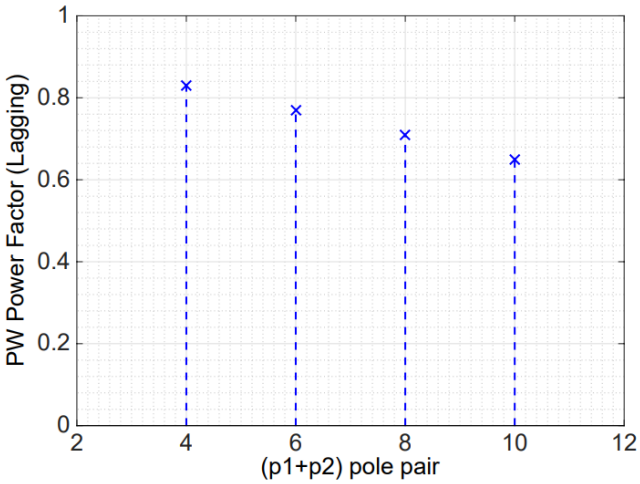

Fig. 6: PW power factor variation with sum of pole-pairs at rated torque and speed.

D. Efficiency

Figure. 7, shows the variation of efficiency as the PW power factor is improved for the existing 250 kW brushless DFIG prototype. Achieving a higher PW power factor comes at a price of reduced efficiency, illustrating the trade-off between satisfying power factor requirements and other performance measures.

VII. Megawatt Machines

The intention is, of course, to deploy the brushless DFIG in large wind turbines so it is important to know how such a machine would operate. According to recent grid codes, wind farms have to supply reactive as well as real power to the grid. For a brushless DFIG the power factor can be controlled by

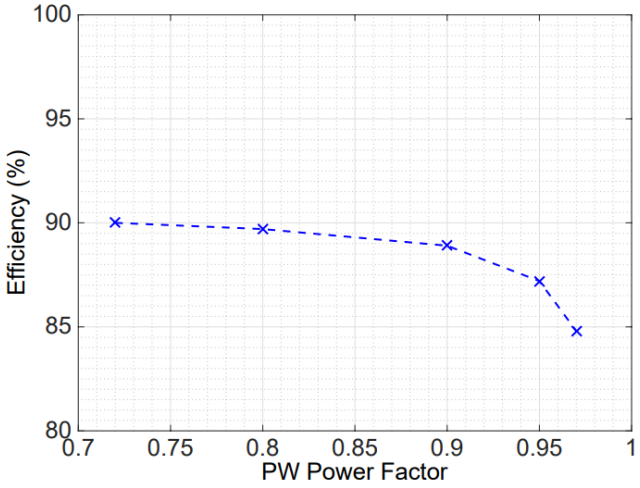

Fig. 7: Efficiency variation with PW power factor for 250 kW brushless DFIG.

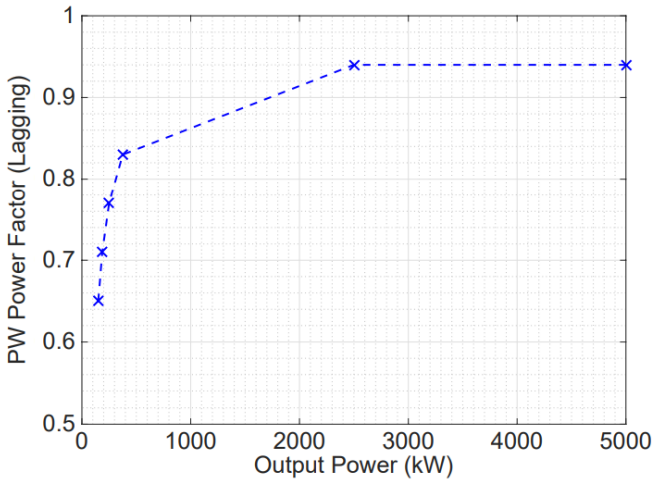

Fig. 8: PW power factor variation with sum of pole-pairs at rated torque and speed.

the converter feeding the control winding but as noted in [17] there are practical limits. To explore the expected performance of large machines, designs have been developed for 2.5 and 5 MW medium speed machines as tabulated in Tab. VIII. The proportionately lower rotor leakage reactance allows unity PW power factor is achieved in both machines at rated CW design voltages without increasing B_{sum} which therefore has been kept at 0.7 T.

TABLE VIII: Optimized Design for MW Brushless DFIGs

Brushless DFIG design parameters		
	2.5 MW	5 MW
Pole (p_1/p_2)	4/8	8/12
Stack length (mm)	920	800
Air gap diameter (mm)	1065	1965
ω_n (rpm)	500	300
Speed range (rpm)	320-680	192-408
Rated power (MW)	2.5	5
Rated PW voltage (V)	690 at 50 Hz	690 at 50 Hz
Rated CW voltage (V)	660	620
Rotor slots	60	140
Stator slots	72	72
B_1 (T)	0.275	0.290
B_2 (T)	0.425	0.410
N_1	18	20
N_2	72	52
Efficiency	96%	97%
Torque (kNm)	38.4	120
PW power factor	1	1
Total amp turns	6542	8020

Figure. 8, shows changes of the PW power factor for rated torque and speed operation as machine size increases. The machines are taken from Tab. V and Tab. VIII, noting that they have different pole numbers. Each data point was recorded for a balanced excitation condition, with each winding providing its own magnetizing current. This condition was achieved by adjusting the CW voltage to minimize the rotor currents, for a given PW voltage, at full load operating conditions.

It is evident that smaller machines suffer from lower power factors without an excessively high CW voltage. A line side converter with a higher rating or capacitor banks at grid terminals can be used to contribute to the generation of reactive power. However, for larger machines, the per unit value of the rotor reactance drops with size [22] therefore, higher factors can be acheieved without greatly increasing CW voltage. For MW scale machines, a worst case PW power factor of 0.95 lagging is achieved at balanced excitation and a modest degree of over-excitation of the CW will enable the export of VArs to the grid.

VIII. Conclusion

This paper considers the design of the brushless DFIG starting with the choice of pole-pair numbers to set the speed. Analysis shows that the theoretical torque capability of a brushless DFIG has a weak dependence on pole numbers, with better performance obtainable with more widely separated values. The pull-out torque capability falls with rising pole number count but an acceptable value is achievable with these slower speed machines; the choice of pole-pair numbers, if different options are available is not critical. The back iron depth has a weak dependence on pole number count and the ratio of the two pole-pair numbers, with lower values for less widely spaced pole-number values. Magnetization follows the same trend but when the output factor is considered, all brushless DFIGs require essentially the same magnetizing AT as a corresponding DFIG. The same trends are evident whether the simple sum or quadrature sum of fields is used; finite element analysis is likely to lead to a design between the two boundaries. A designer will also consider harmonic production and vibration.

On the basis that peak flux densities can be increased without undue saturation, it has been shown that a higher output power factor in an existing 250 kW 4-pole/8-pole machine can be achieved without undue over-excitation of the control winding. Consideration has also been given to the expected performance of multi-megawatt machines and it

is predicted that acceptable performance at a leading power factor can be achieved.

APPENDIX A

The power rating of the brushless DFIG, calculated from the equivalent circuit model, was derived in [1] based on the quadrature sum of fields and is given by:

$$P_{quad} = \frac{\pi^2}{\sqrt{2}}\left(\frac{d}{2}\right)^2 l\omega_r \overline{BJ}\left[\frac{p_1+p_2}{p_1(1+\frac{1}{n_r})(1+\left(n_r\frac{p_2}{p_1})^2\right)^{\frac{1}{2}}}\right] \tag{16}$$

The power rating of a conventional induction machine with $(p_1 + p_2)$ pole-pairs is found from:

$$P_{IM} = \frac{\pi^2}{\sqrt{2}}\left(\frac{d}{2}\right)^2 l\overline{BJ}\left[\frac{\omega_s}{p_1+p_2}\right] \tag{17}$$

The output power is then calculated as:

$$\frac{P_{quad}}{P_{IM}} = \left[\frac{p_1+p_2}{p_1(1+\frac{1}{n_r})(1+(n_r\frac{p_2}{p_1})^2)^{\frac{1}{2}}}\right] \tag{18}$$

Using the alternative B_{sum} approach, for the brushless DFIG, maximum output power can be calculated as:

$$P_{B_{sum}} = \frac{\pi^2}{\sqrt{2}}\left(\frac{d}{2}\right)^2 l\omega_r \overline{BJ}\left[\frac{1}{p_1(1+\frac{1}{n_r})+(1+n_r\frac{p_2}{p_1})}\right] \tag{19}$$

Hence, output power ratio is then calculated as:

$$\frac{P_{B_{sum}}}{P_{IM}} = \left[\frac{p_1+p_2}{p_1(1+\frac{1}{n_r})+(1+n_r\frac{p_2}{p_1})}\right] \tag{20}$$

These powers can be normalised to the output of a $p_1 + p_2$ DFIG leading to output factor of:

$$Outputfactor = \frac{T_{BDFIG}}{T_{IM}}\left[\frac{1+\frac{p_2}{p_1}}{(1+\frac{1}{n_r})(1+\left(n_r\frac{p_2}{p_1}\right)^2)^{\frac{1}{2}}}\right] \tag{21}$$

For the quadrature sum method and:

$$Outputfactor = \frac{T_{BDFM}}{T_{IM}}\left[\frac{1+\frac{p_2}{p_1}}{1+\frac{1}{n_r}+\frac{p_2}{p_1}(1+n_r)}\right] \tag{22}$$

for the sum method.

The $n_{r_{opt}}$ is defined using the method given in [1], with the assumption of unity power factor and small load angle operation. The turns ratio for maximum output power is given by:

$$n_{r_{opt}} = \left(\frac{p_1}{p_2}\right)^{\frac{1}{2}} \tag{23}$$

However, this is constant to the results obtained in [1]:

$$n_{r_{opt}} = \left(\frac{p_1}{p_2}\right)^{\frac{2}{3}} \tag{24}$$

The actual value of $n_{r_{opt}}$ are 0.71 and 0.63 for the 4/8 brushless DFIG from equation (23) and (24).

ACKNOWLEDGMENT

The research leading to these results has received funding from the European Union's Seventh Framework Program managed by Research Executive Agency (FP7/2007-2013) under Grant Agreement N.315485.

REFERENCES

[1] R. McMahon, X. Wang, E. Abdi, P, Tavner, P. Roberts and M. Jagiela, "The brushless DFIG as a generator in wind turbines," *Power Electronics and Motion Control Conference*, Slovenia, pp. 1859 – 1865, 2006. doi: [sa9]

[2] T. Strous, X. Wang, H. Polinder, and J. Ferreira, "Brushless doubly fed induction machines: magnetic field analysis," *IEEE Transactions on Magnetics*, VOL. 52, NO. 11, November 2016. doi: 10.1109/TMAG.2016.2587879. [sa1]

[3] B. Gorti, G. Alexander and R. Spee. A novel, cost-effective stand-alone generator system. IEEE 4th AFRICON, September 1996. doi: 10.1109/AFRCON.1996.562962. [sa2]

[4] B. V. Gorti, G. C. Alexander, R. Spee, and A. K. Wallace. Microcontroller based efficiency maximization for a brushless doubly-fed machine pump drive. IEEE/IAS International Conference on Industrial Automation and Control, January 1995. doi: 10.1109/IACC.1995.465811. [sa5]

[5] A. K. Wallace, R. Spee, and H. K. Lauw. The potential of brushless doubly-fed machines for adjustable speed drives. pages 45 – 50. IEEE Conference Record of the Pulps and Paper Industry Technical Conference, June 1990. doi: 10.1109/PAPCON.1990.109862. [sa7]

[6] F. Xiong and X. Wang., "Design and performance analysis of a brushless doubly-fed machine for stand-alone ship shaft generator systems." International Conference on Electrical and Control Engineering (ICECE), September 2011. doi: 10.1109/ICECENG.2011.6057462. [sa10]

[7] R. Rebeiro and A. Knight, "Design and torque capability of a ducted rotor brushless doubly fed reluctance machine", IET Electr. Power Appl., Vol. 12 Iss. 7, pp. 1058-1064, August 2018. doi: 10.1049/iet-epa.2017.0759 [sa11]

[8] T. Staudt, F. Wurtz, L. Gerbaud, N. Batistela and P. Kuo-Peng, "An optimization-oriented sizing model for brushless doubly fed reluctance machines: Development and experimental validation", Electric Power System Research, Elsevier, pp. 125-131, December, 2016. doi.org/10.1016/j.epsr.2015.10.029. [sa8]

[9] T. Strous, H. Polinder and J. Ferreira, "Brushless doubly-fed induction machines for wind turbines: developments and research challenges" IET Electric Power Applications, Vol. 11, Iss. 6, pp. 991–1000, July 2017.doi: 10.1049/iet-epa.2016.0118. [2]

[10] X. Wang, R. McMahon, and P. Tavner, "Design of the brushless doubly-fed induction machine," *in Electric Machines Drives Conference, IEEE International*, vol. 2, pp. 1508–1513, May 2007. doi: 10.1109/IEMDC.2007.383651 [3]

[11] R. McMahon, E. Abdi, P. Malliband, S. Shao, M. E. Mathekga, and P. Tavner, "Design and testing of a 250 kW medium-speed brushless DFIG," *in Power Electronics, Machines and Drives, 6th IET International Conference on*, pp. 1–6, March 2012. doi: 10.1049/cp.2012.0320. [4]

[12] F. Runcos, R. Carlson, N. Sadowski, P. Kuo-Peng, and H. Voltolini, "Performance and vibration analysis of a 75 kW brushless double-fed induction generator prototype," *in Industry Applications Conference, 41st IAS Annual Meeting. Conference Record*, vol. 5, pp. 2395–2402, Oct 2006. doi: 10.1109/IAS.2006.256876. [5]

[13] A. Oraee, E. Abdi, S. Abdi and R. A. McMahon, "A study of converter rating for the brushless DFIG," *in Renewable Power Generation Conference*, pp. 1–4, September 2013. doi: 10.1049/cp.2013.1848. [6]

[14] H. Liu, L. Xu, "Design and performance analysis of a doubly excited brushless machine for wind power generator application," *IEEE Int. Symp. Power Electronics for Distributed Generation Systems*, June 2010. doi: 10.1109/PEDG.2010.5545871. [7]

[15] E. Abdi, R. McMahon, P. Malliband, S. Shao, M. Mathekga, P. Tavner, S. Abdi, A. Oraee, T. Long and M. Tatlow, "Performance analysis and testing of a 250 kW medium-speed brushless doubly-fed induction generator," *IET Renewable Power Generation*, vol. 7, pp. 631-638, 2013. doi: 10.1049/iet-rpg.2012.0234. [8]

[16] A. Oraee, E. Abdi, S. Abdi, R. McMahon and P. Tavner, "Effect of rotor winding structure on the BDFM equivalent circuit parameters," *IEEE Transactions on Energy Conversion*, vol. PP, no. 99, pp. 1-10, 2015. doi: 10.1109/TEC.2015.2432272.
[9]

[17] A. Oraee, E. Abdi, R. McMahon, "Converter rating optimization for a brushless doubly fed induction generator," *IET Renewable Power Generation*, vol. 9, no. 4, pp. 360-367, 2015. doi: 10.1049/iet-rpg.2014.0249. [10]

[18] R. McMahon, M. Mmamolatelo, W. Xiaoyan and M. Tatlow, "Design considerations for the brushless doubly-fed induction machine," *IET Electric Power Application*, vol. 10, no. 5, pp. 394–402, June 2016. doi: 10.1049/iet-epa.2015.0405. [11]

[19] S. Abdi, E. Abdi and R. McMahon, "Optimization of the magnetic circuit for brushless doubly fed machines," *IEEE Transactions on Energy Conversion*, vol. 30, no. 4, pp. 1611-1620, 2015. doi: 10.1109/TEC.2015.2468063. [12]

[20] R. McMahon, P. C. Roberts, M. Tatlow, E. Abdi, A. Broekhof and S. Abdi, "Rotor parameter determination for the brushless doubly fed induction machine," *IET Electric Power Applications*, vol. 9, no. 8, pp. 549-555, September 2015. doi: 10.1049/iet-epa.2015.0023 [13]

[21] A. Broadway and L. Burbridge, "Self-cascaded machine: a low-speed motor or high frequency brushless alternator," *Proceedings, Institution of Electrical Engineers*, vol. 117, pp. 1227–1290, 1970. doi: 10.1049/piee.1970.0247. [14]

[22] S. Tohidi, P. Tavner, R. McMahon, M. Zolghadri, S. Shao and E. Abdi, "Low voltage ride-through of DFIG and brushless DFIG: similarities and differences," *Electric Power Systems Research*, 110, pp. 64–72, May 2014. doi: 10.1016/j.epsr.2013.12.018.